2000

Magnetic coupling in neutral and charged Cr-2, Mn-2, and CrMn dimers

N. Desmarais
École polytechnique fédérale de Lausanne (EPFL)

F. A. Reuse
École polytechnique fédérale de Lausanne (EPFL)

S. N. Khanna
Virginia Commonwealth University

Magnetic coupling in neutral and charged Cr_2, Mn_2, and CrMn dimers

N. Desmarais[a] and F. A. Reuse
Institut de Physique Expérimentale, Ecole Polytechnique Fédérale de Lausanne, PHB-Ecublens, CH-1015 Lausanne, Switzerland

S. N. Khanna
Department of Physics, Virginia Commonwealth University, Richmond, Virginia 23284-2000

(Received 18 October 1999; accepted 21 December 1999)

Theoretical *ab initio* studies of neutral, cationic and anionic Cr_2, Mn_2, and CrMn dimers have been carried out to explore the progression of magnetic coupling with the number of electrons. It is shown that while Cr_2 and Cr_2^- have antiferromagnetically coupled atomic spins, Cr_2^+ has a ferromagnetic ground state closely followed by an antiferromagnetic state. On the other hand, all Mn_2 dimers are ferromagnetic, irrespective of the charge. The neutral CrMn is ferrimagnetic while the charged CrMn are antiferromagnetic. In all cases, the charged dimers are found to be more stable than the neutral ones. The results are compared with available calculations and experiments and the difficulties associated with theoretical description and the experimental interpretations are discussed. © *2000 American Institute of Physics.* [S0021-9606(00)30311-7]

I. INTRODUCTION

Cr and Mn atoms are the only $3d$ atoms with $5d$ electrons and, according to Hunds rules, have a half-filled d shell. The filled subshell leads to intricate magnetic behaviors and even the correct treatment of Cr_2 and Mn_2 dimers has proven to be a challenge to theoretical investigations. For example, for Cr_2, a proper description based on configuration interaction has been estimated to require a large number of configurations (57 million).[1] A modified generalized valence bond (MGVE)[2] approach was proposed to properly account for the correlations. It leads to the antiferromagnetic order and predicted a double-well potential energy surface. The local spin density schemes were generally successful in reproducing the antiferromagnetic order and experimental bond length but lead to a very high binding energy (BE) and could not confirm the double-well potential.[3–5] The situation for Mn_2 has also been interesting. Experiments on Mn_2 molecules in matrices predict an antiferromagnetically coupled dimer.[6–10] Using an approximate Hartree–Fock calculation and an Heisenberg Model, Nesbet has predicted such an antiferromagnetic $^1\Sigma_g^+$ ground state almost 30 years ago.[11] Recent calculations based on density functional theory (DFT), however, predict a ferromagnetic ground state.[12,13] In contrast to Mn_2, experiments on Mn_2^+ in matrices show ferromagnetic coupling with a large magnetic moment (5.5 μ_B per atom)[14] while measurements on CrMn dimers in matrices gives a net spin of 1.5 indicating ferrimagnetic or ferromagnetic coupling.[10]

In this paper we report results of density functional (DF) calculations on Cr_2, Mn_2, and CrMn dimers and their charged counterparts. Our objective is twofold. (1) To examine the applicability of the local spin density approximation (LSDA) and generalized gradient approximation (GGA) functionals to these complex molecules. (2) To explore how the nature of magnetic coupling changes as one changes the number of electrons. For each dimer, we investigate the $C_{\infty v}$ and the $D_{\infty h}$ symmetry states to examine the possible magnetic couplings. A Mulliken population analysis is presented to give insight on the magnetic moment distribution at each atomic site (μ_X^M).

In Sec. II we give the details of the calculations and Sec. III contains the results and discussion.

II. COMPUTATIONAL DETAILS

The theoretical scheme used is a linear combination of atomic orbitals (LCAO) approach[15] as implemented within the Kohn–Sham (KS) density functional formalism.[16] The atomic orbitals are expanded in terms of gaussian functions centered at the atomic sites. Furthermore, the charge density and the exchange correlation potentials and energy density are fitted with sets of auxilliary gaussian functions centered at the nucleus. For details the reader is referred to our earlier paper.[17] Calculations were performed at the all-electron level using large uncontracted gaussian basis sets fully optimized for density functional calculations: the DZVP2[18] basis set $(15s/9p/5d)$. Exchange and correlation contributions have been treated at two levels namely the LSDA and the GGA. For LSDA calculations, we have used the form proposed by Perdew and Wang (PW91)[19] while for GGA, the recent functional of Perdew, Burke, and Ernzerhof (PBE96)[20] was used. Fractional occupation numbers were used (via a small electronic temperature) whenever the highest occupied molecular orbital (HOMO) was degenerate. The final results, however, always correspond to zero temperature and have integral occupation numbers. Unless otherwise specified, the multiplet problem[21] was not treated here. Our computed energies, thus represent, an average value over all pure spin states (from $S=m_S$ up to $S_{\max}$, the latter being formerly defined by the total number of electrons but in practice only the outer shell electrons really contribute).

[a]Electronic mail: khanna@hsc.vcu.edu

TABLE I. Calculated atomic ionization potential (IP), electronic affinity (EA), and total spin value (m_S) along with their experimental counterpart and predicted state.

	IP (eV)			EA (eV)				
Atom	LSDA	GGA	Expt.[a]	LSDA	GGA	Expt.[b]	m_S	Expt. State[a]
Cr	7.53	7.35	6.766	0.56	0.28	0.666	3	$^7S_3$
Mn	7.52	7.18	7.435	−0.29	−0.60	[c]	2.5	$^6S_{2(1/2)}$

[a]From Ref. 48.
[b]From Ref. 49.
[c]Mn^- is not observed.

In this paper, m_S will refer to the difference between the number of up and down electrons divided by 2 and will be called the total or net spin value. The, so defined, spin value is the eigenvalue of the operator $\hat{\mathbf{S}}_z$ applied on the one determinant wave function of the reference Kohn–Sham noninteracting system. On the other hand, S will refer to the spin value of the real eigenstate of the system. We might sometimes call ''singlet,'' ''triplet'' and so forth, the $m_S = 0,1,...,$ KS solutions, although these solutions are contaminated by higher spin states and do not usually represent the real spin state to which they refer. We also define the localized spin moment, μ_X^M (where the index M underline the relationship to the arbitrary decomposition scheme of Mulliken), as the difference between the up and down Mulliken population at a given site, X. This term gives a qualitative insight of the magnetic moment distribution at each atomic site.

III. RESULTS AND DISCUSSION

Our results on atoms are given, for completeness, in Table I. The calculated ionization potential (IP) based on LSDA and GGA show fairly good agreement with experiment. For the Cr atom the LSDA electronic affinities (EA) agrees better than GGA. Both functionals lead to an unstable Mn^- anion in agreement with available experimental results.

Table II gives the ground state bond length, total spin value, binding energy and localized spin moment per atom for all neutral and charged dimers. Note that the binding energy of the anionic and cationic species are computed relative to the corresponding neutral and charged atom. Negative binding energy indicate an unstable dimer. For the charged CrMn dimers, based on the theoretical IP and EA of free atoms, we choose the dissociation channel $CrMn^+ \rightarrow Cr + Mn^+$ and $CrMn^- \rightarrow Cr^- + Mn$. The variations with the net spin multiplicity of PBE96 bond length, binding energy and localized spin moment per atoms are reported in Figs. 1–9 for the neutral, cationic, and anionic, Cr_2, Mn_2, and CrMn dimers. The open circle in the magnetic moment part of each figure indicates the magnetic moment on one atom while the dots indicate the magnetic moment on the

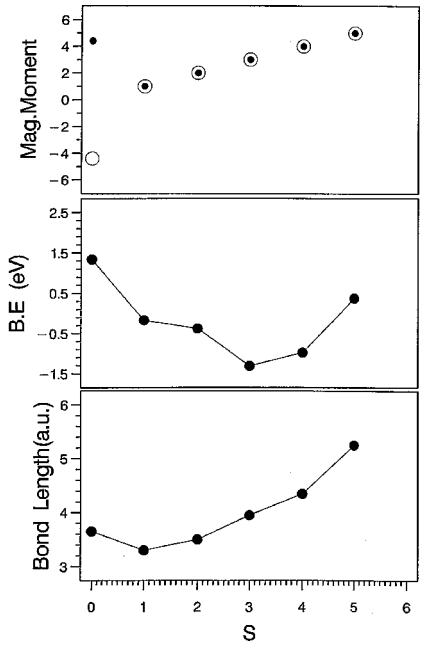

FIG. 1. Bond length, binding energy, and the spin magnetic moment at the two atomic sites (marked by hollow and filled circles) in Cr_2.

TABLE II. GGA(PBE96) equilibrium bond length (r_e) binding energy (BE), net spin (m_S), magnetic coupling (MC), and spin magnetic moment per site (μ_X and μ_Y) for all XY neutral and charged dimers (X,Y=Cr or Mn). LSDA(PW91) results are given in square brackets.

XY	r_e(a.u.)	BE (eV)	m_S[a]	MC[a,b]	μ_X[c] (μ_B)	μ_Y[c] (μ_B)
Cr_2	3.64[3.22]	1.34[2.35]	0.0	AF	+4.40[+2.80]	−4.40[−2.80]
Cr_2^+	5.60[3.15]	1.54[2.47]	5.5	FM	+5.50[+2.70]	+5.50[−1.70]
Cr_2^-	3.65[3.30]	1.40[2.25]	0.5	AF	+4.30[+3.05]	−3.30[−2.05]
Mn_2	4.95[4.75]	0.63[0.84]	5.0	FM	+5.00[+5.00]	+5.00[+5.00]
Mn_2^+	5.60[4.60]	1.63[1.91]	5.5	FM	+5.50[+5.50]	+5.50[+5.50]
Mn_2^-	4.40[4.35]	1.67[1.88]	4.5	FM	+4.50[+4.50]	+4.50[+4.50]
CrMn	4.30[4.00]	0.82[1.37]	0.5	FIM	+5.25[+4.85]	−4.25[−3.85]
$CrMn^+$	4.25[4.00]	2.33[2.90][d]	0.0	AF	+5.00[+4.70]	−5.00[−4.70]
$CrMn^-$	4.80[4.05]	1.18[1.61][e]	0.0	AF	+4.55[+4.10]	−4.55[−4.10]

[a]LSDA net spin (m_S) and magnetic coupling (MC) are identical to their GGA counterpart for all dimers except Cr_2^+ (in which case, $m_S=0.5$, MC=AF).
[b]The magnetic coupling symbols used are AF (antiferromagnetic), FM (ferromagnetic), and FIM (ferrimagnetic).
[c]A ''+'' (''−'') sign indicates a majority of up (down) spin.
[d]Dissociation channel: $CrMn^+ \rightarrow Cr + Mn^+$.
[e]Dissociation channel: $CrMn^- \rightarrow Cr^- + Mn$.

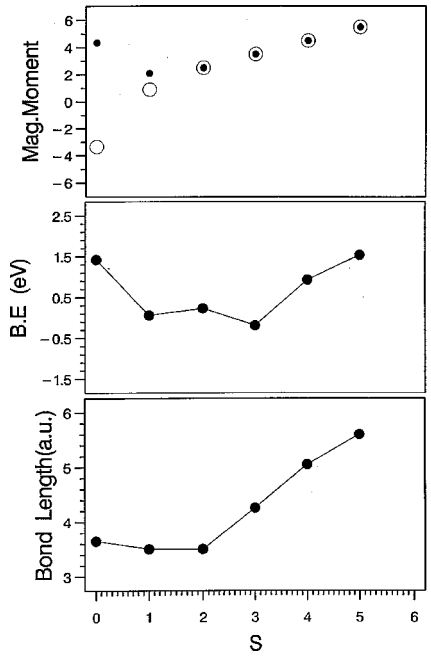

FIG. 2. Bond length, binding energy, and the spin magnetic moment at the two atomic sites (marked by hollow and filled circles) in Cr_2^+.

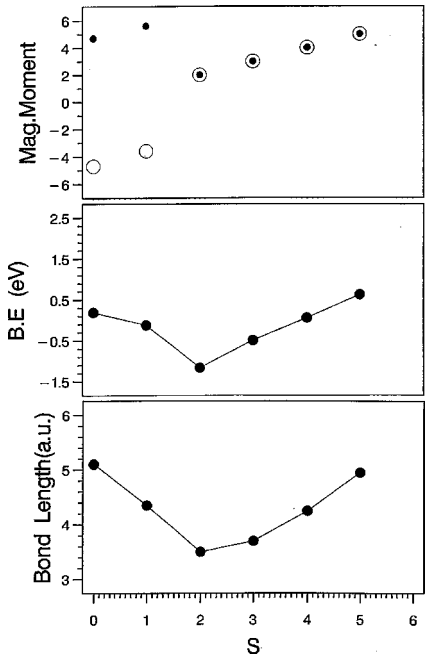

FIG. 4. Bond length, binding energy, and the spin magnetic moment at the two atomic sites (marked by hollow and filled circles) in Mn_2.

other atom. This give us a clear picture of the magnetic coupling involved. Each dimer result will be discussed in detail in the following sections.

A. Neutral and charged chromium dimers

We begin with our results on neutral Cr_2 which has been the subject of several experimental[22–24] and theoretical[2–4,25–28] investigations. LSDA calculations were the first to obtain a bond length (3.17–3.22 a.u.) in good agreement with the experimental one while overestimating the binding energy (1.80–2.8 eV).[3,4,26] Goodgame and Goddard using a modified generalized valence bond (MGVB) scheme found a reasonable estimate of both the bond length and the binding energy (3.04 a.u. and 1.86 eV).[2] They also found a second minima at 5.78 a.u. bound by 0.3 eV only. More recently, Andersson *et al.*[27] using a CASPT2 scheme obtained a very good agreement with the experimental results: $r_e = 3.23$ a.u., BE$=1.54$ eV. They also observe a second minima around 4.5–5.0 a.u., which become a shelf upon inclusion of relativistic corrections. At the same time, Baus-

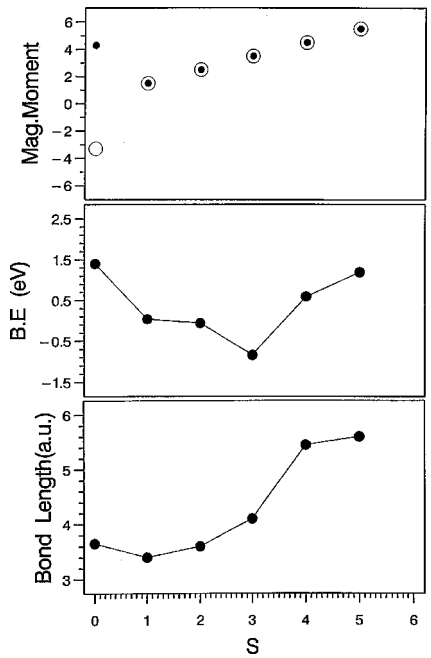

FIG. 3. Bond length, binding energy, and the spin magnetic moment at the two atomic sites (marked by hollow and filled circles) in Cr_2^-.

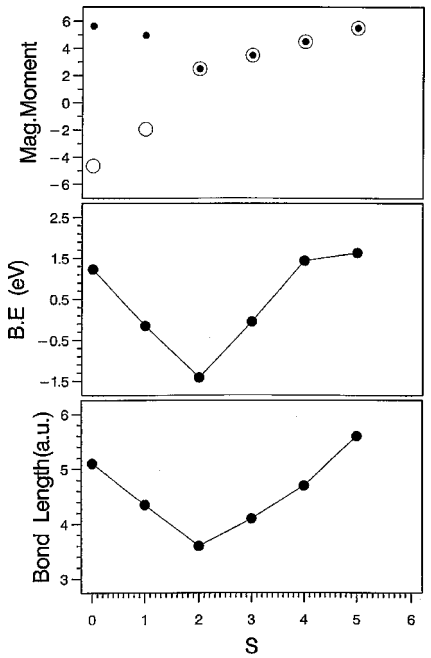

FIG. 5. Bond length, binding energy, and the spin magnetic moment at the two atomic sites (marked by hollow and filled circles) in Mn_2^+.

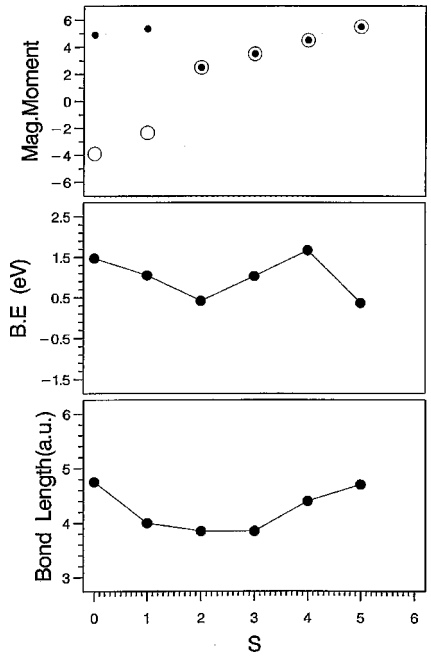

FIG. 6. Bond length, binding energy, and the spin magnetic moment at the two atomic sites (marked by hollow and filled circles) in Mn_2^-.

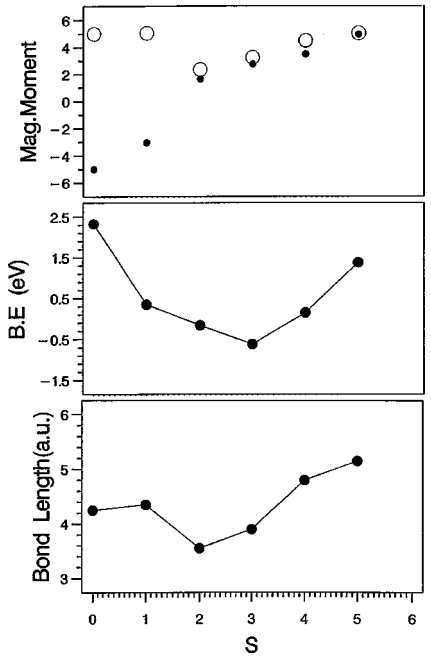

FIG. 8. Bond length, binding energy, and the spin magnetic moment at the two atomic sites (marked by hollow and filled circles) in $CrMn^+$.

chlicher and Partridge[28] have performed coupled cluster single double (CCSD) calculations and DFT-GGA calculations using the Becke–Lee–Yang–Parr (BLYP) functional and the three parameters hybrid functionals of Becke (B3LYP, B3P86, see Ref. 28 and References therein for more details). The CCSD, B3LYP, and B3P86 calculations failed, giving too large of a bond length (around 4.75 a.u.) and too small binding energy (approximately 1 eV), while the BLYP functional leads to a reasonable bond length (3.21 a.u.) but overestimate the binding energy (1.99 eV). Edgecombe and Becke[25] have used a simple scheme to extract the pure singlet energy from the broken symmetry and highest spin state KS energies for the LSDA (VWN), B3LYP, and B3P86 functionals. We will come back to their results later on, but for now we just want to point out that the notation SP-XYZ will designate the ''spin projected'' (SP) pure singlet, where XYZ stands for the ''XYZ'' functional.

In Table III we compare our calculated bond length, binding energy, and total spin value with previous calculations and experiment. Second minimum, or shelf, are also

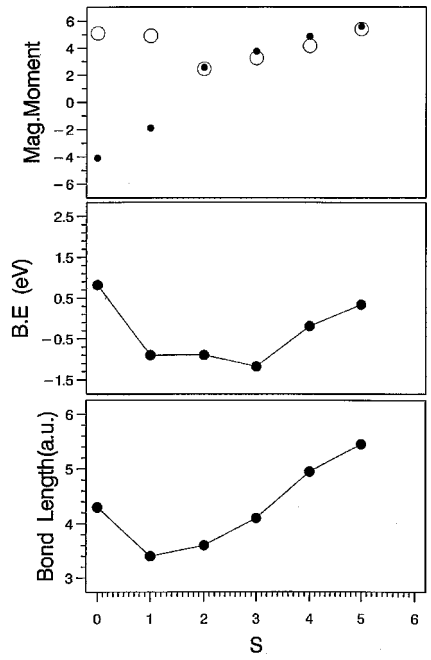

FIG. 7. Bond length, binding energy, and the spin magnetic moment at the two atomic sites (marked by hollow and filled circles) in CrMn.

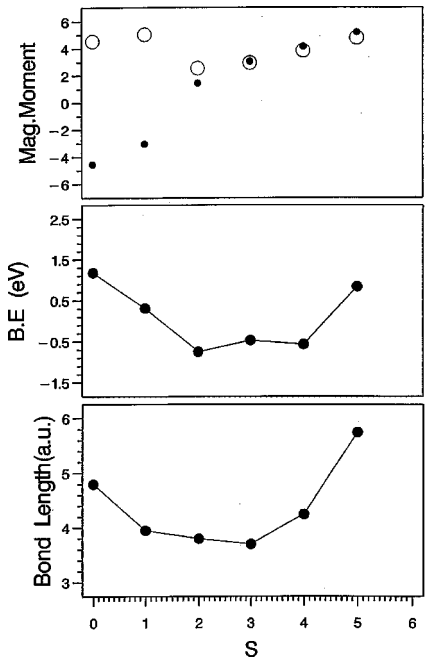

FIG. 9. Bond length, binding energy, and the spin magnetic moment at the two atomic sites (marked by hollow and filled circles) in $CrMn^-$.

TABLE III. Calculated and experimental equilibrium bond length (r_e), harmonic frequency (ω_e), binding energy (BE), and total spin value (m_S) or electronic state of neutral chromium dimer.

	r_e	ω_e	BE	m_S/state
LSDA(BH)[a]	3.21	450	1.80	0
LSDA(VWN)[b]	3.17	441	2.6	0
LSDA(VWN)[c]	3.17		2.28	0
BLYP[d]	3.21		1.99	0
B3LYP[d]	4.74		1.07	0
B3P86[d]	4.76		0.98	0
SP-B3P86[e]	1.59		1.38	Singlet
	2.40		1.14	
MGVB[f]	3.04		1.86	$^1\Sigma_g^+$
	5.78		0.3	
CASPT2[g]	3.25	596	1.37	$^1\Sigma_g^+$
	4.5–5.0			
CASPT2+RC[g]	3.24	625	1.54	$^1\Sigma_g^+$
	4.5–5.0			
LSDA(PW91)[h]	3.22	392	2.35	0
PBE96[h]	3.64	365	1.34	0
	4.15		1.15	
Expt.	3.17[i]	480.6±0.5[j]	1.42±0.10[k]	$^1\Sigma_g^+$
	4.35–5.48			

[a]Results from Ref. 3. BH: Barth and Hedin functional (Ref. 50).
[b]Results from Ref. 4. VWN: Vosko, Wilk, and Nusair functional (Ref. 51).
[c]Results from Ref. 26. VWN: Vosko, Wilk, and Nusair functional (Ref. 51).
[d]Results from Ref. 28. BLYP: Becke exchange (Ref. 52) and Lee–Yang–Parr correlation functionals (Ref. 53), B3LYP, B3P86: Becke 3 parameters functionals (Ref. 54).
[e]Results from Ref. 25. SP-B3P86: spin projected singlet using the B3P86 functional.
[f]Results from Ref. 2. MGVB: modified generalized valence-bond methods.
[g]Results from Ref. 27. CASPT2: complete active space second order perturbation theory. CASPT2+RC: CASPT2+relativistic corrections.
[h]Present work.
[i]From Ref. 22.
[j]From Ref. 24.
[k]From Ref. 23.

reported when available. It is well known[3,4] that, in KS-DFT, one has to carry out broken symmetry calculations on such antiferromagnetic systems. It is thus intriguing to note that, in their recent paper, Cheng *et al.*[26] have used $D_{\infty h}$ symmetry. Such a symmetry has lead to a zero local magnetic moment at the Cr sites as opposed to $\mu_{\mathrm{Cr}}^M = 4.40\,\mu_B$ obtained here. In the last column of Table III the electronic state is reported for MGVB and CASPT2 methods while, due to the multiplet problem,[21] only the total spin value, m_S, is reported for DF based methods.

The present results are reported under the labels LSDA (PW91) and PBE96. Note that while PW91 gives a bond length close to the experimental value, the binding energy is strongly overestimated. These results are in good agreement with other broken symmetry LSDA calculations. PBE96, on the other hand, leads to a larger bond length but gives a reasonable estimate of the binding energy. Interestingly, the GGA potential curve shows a second minima at 4.15 a.u. with a binding energy of 1.15 eV in addition to the ground state. The existence of this minima is particularly significant in view of the experiments by Casey and Leopold[24] which do indicate the existence of a shelf (or possibly a minimum) around 4.35–5.48 a.u. But as can be seen in Fig. 11, the PBE96 functional fails to correctly reproduce the entire potential curve. In this figure, we show the potential energy curve for Cr_2 based on present calculations (PBE96) and on CASPT2+RC,[27] MGVB,[2] DFT BLYP, B3LYP,[28] and DFT SP-B3P86 (Ref. 25) calculations. The experimental RKR curve, obtained from a fit of 30 vibrational levels,[24] is also reported. Note that, except for CASPT2+RC which gives a good overall description, all the other methods, including the present calculations, fail to reproduce the entire potential curve. LSDA curves, which are not reported for cumbersome reasons, are similar to the BLYP one. It is thus clear that in this case, the PBE96 functional, as well as other GGA based functionals, do not generally improve LSDA results. Furthermore, while all LSDA results show the same trends (reasonable bond length, overestimate the binding energy, no double well), GGA results can be quite different from each others. One would generally assume that GGA functionals better describe the exchange and correlation hole than LSDA ones. This would imply that LSDA results were good for the wrong reasons. On the other hand, since different GGA functionals show different behaviors, it may indicate that rather than improving LSDA results, they erroneously treat the delicate interplay between bonding and magnetic coupling found in chromium dimer. It would certainly be interesting for future development to have a good understanding of what goes wrong in each case.

We now come back to the result of Edgecombe and Becke. The ground state obtained here is based on a broken symmetry, spin unrestricted, density functional theory. Such a ground state has spin contamination and it is desirable to compare results with pure spin singlet states. A simple approach to calculate spin singlet energies using the broken symmetry and the maximum spin energies has been proposed by Noodleman.[29] The proposed scheme assumes weak coupling of the atoms and implies the validity of the Heisenberg model. It has been used by Edgecombe and Becke[25] to calculate the spin uncontaminated singlet ground state. Their results based on the B3P86 hybrid functional do exhibit a double-well potential energy curve with minima at 3.00 and 4.53 a.u. bound by 1.38 and 1.14 eV, respectively. While the existence of double minima and their binding energy are in agreement with the present work and the deduced experimental curve, the calculations of Edgecombe and Becke have severe limitations. The scheme proposed by Noodleman is valid only for weak coupling where there is negligible overlap, S_{ab}, between the atoms carrying the localized spins such as in transition metal complexes.[29] This is certainly not the case for Cr_2 which has a short bond length. In addition, as shown in Table II the localized moments at the atomic sites are much different from their free atom values. In such cases, i.e., where the overlap integral is not small, it has been shown that the application of this scheme can lead to severe errors.[30] The error is proportional to S_{ab} and thus the validity of this technique for short bond range is questionable. In obtaining the spin uncontaminated ground state from the broken symmetry solution, Edgecombe and Becke used a maximum spin of $S_{\max}=5$ whereas the dimer actually has a maximum spin of $S_{\max}=6$. The authors have also calculated spin projected curves for the VWN and BLYP functionals. Both curves show shorter equilibrium bond length and none of

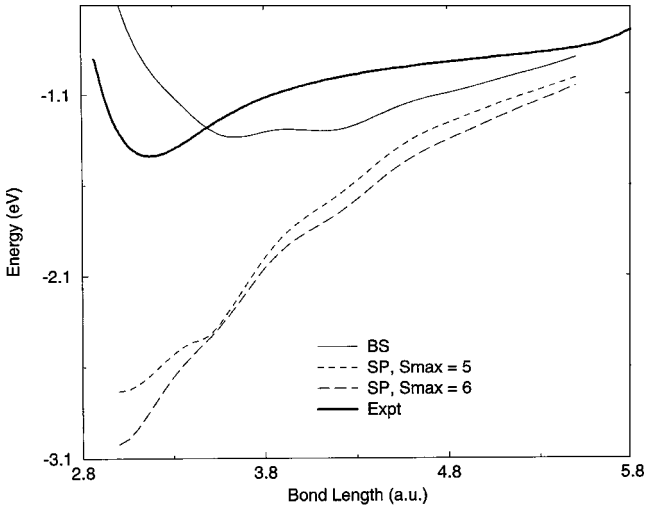

FIG. 10. Broken symmetry (BS), and spin projected (SP) singlet potential energy curves obtained with the PBE96 functional for the chromium dimer. The SP curve is given for two values of $S_{\max}$. The experimental curve is added for comparison.

them show better agreement with the deduced experimental curve. In fact, the agreement is worse. We tried to calculate the pure spin singlet energy using the present broken symmetry and maximum spin energies within the Noodleman scheme. The results are shown in Fig. 10 for the PBE96 functional with $S_{\max}=5$ (for comparison with Becke work) and $S_{\max}=6$ [the same general trends are observed with the LSDA (PW91) functional, but the curves are not reported here]. Note that the spin projected singlet state collapses to a short bond length and the second minima becomes a shoulder. The value of the Heisenberg exchange integral around the broken symmetry equilibrium distance is $J \approx -1300\,\mathrm{cm}^{-1}$ (≈ -0.16 eV) for both spin projected singlet. This value decreases with shorter bond length. Finally, we argue that the Noodleman scheme cannot be used for Cr_2 because it implies a weak coupling between the atoms and the validity of the Heisenberg model. It would rather be interesting to use methods based on the line of the work of Ziegler *et al.*[21] to see how the BS potential energy curve is affected.

For Cr_2^+, the PBE96 predicts a ferromagnetic ground state ($\mu=11\,\mu_B$) with a bond length of 5.60 a.u. and a binding energy of 1.54 eV. This state is only 0.015 eV more stable than an antiferromagnetic state ($\mu=1\,\mu_B$) with a bond length of 4.22 a.u. The LSDA (PW91), on the other hand, predicts an antiferromagnetic configuration ($\mu=1\,\mu_B$) with a bond length of 3.15 a.u. and a binding energy of 2.47 eV. This state is 0.89 eV more stable than the ferromagnetic state ($\mu=11\,\mu_B$) which has a bond length of 5.35 a.u. This is the only qualitative disagreement between LSDA (PW91) and PBE96 results. Recent experiments[23] estimate the binding energy of Cr_2^+ to be 1.30 eV in good agreement with the PBE96 result. In the case of Cr_2^-, however, both the GGA and the LSDA predict an antiferromagnetic ground state with a net spin of 0.5 which is consistent with the experimental doublet ground state.[24] The calculated bond length of 3.65 (3.30) a.u. and the electron affinity of 0.34 (0.46) eV within the PBE96 (LSDA (PW91)) are comparable to the experimental estimates[24] of 3.22 a.u. and 0.50 eV, respectively. From Fig. 1 we see that the evolution of the relative stability of the different spin state of neutral chromium dimer is not linear neither quadratic but rather it exhibit a *U*-kind of shape while the variation of the bond length with m_S is almost linear. This, as we have said, support the non applicability of the Heisenberg model to this system. Figures 2 and 3 show that the charged dimers relative energies with spin also exhibit a strange shape, while the variation of bond length is almost regular.

B. Neutral and charged manganese dimers

We now consider the magnetic coupling in Mn_2 clusters. The nature of magnetic coupling in small Mn_n ($n=2-8$) clusters has been recently investigated by the present and other authors.[12,13] It was shown that while the bulk α-Mn is antiferromagnetic, small Mn_n clusters are ferromagnetic with large magnetic moments. The case of Mn_2 has been of particular interest since the electron spin resonance (ESR) on Mn_2 in matrices predict a weakly bound ($\approx$6.42 a.u.) antiferromagnetic molecule with an Heisenberg exchange integral of $J=-9\pm3\,\mathrm{cm}^{-1}$.[6,8–10] This result was confirmed by UV absorption. Based on the assumption that the observed absorption band originate from one of the thermally populated low-lying spin states of Mn_2, Rivoal *et al.* have estimated $J=-10\,\mathrm{cm}^{-1}$.[7] Furthermore, resonance Raman spectroscopy experiments in argon and krypton matrices confirm the existence of a weakly bound manganese dimer with $\omega_e=76.4\,\mathrm{cm}^{-1}$ in krypton.[31] The binding energy was estimated with several methods. Kant *et al.*,[32] based on mass spectrometric analysis and an estimated ''van der Waals'' bond length of 7.18 a.u. and applying the third-law method to their data, have found $D_e(\mathrm{VDW})=0.27\pm0.26$ eV [Haslett *et al.*[33] have pointed out that the original calculated value of the paper (0.33 eV) was erronous]. Haslett *et al.* used the same spectroscopic data with more recent molecular parameters (the estimated bond length of Baumann *et al.* in matrice, $r_e=6.42$ a.u., and their own harmonic frequency, $\omega_e=76.4\,\mathrm{cm}^{-1}$) and have found $D_e(\mathrm{VDW})=0.02$ eV while the application of the LeRoy–Bernstein analyses on resonance Raman data yield $D_e=0.15$ eV. An average of the third-law values give $D_e=0.44\pm0.30$ eV.[34] Morse[35] has suggested to use $D_e\leqslant0.8$ eV to be safe. We are going to stick to his suggestion. The point we would like to underline here, is the fact that the experimental bond length and binding energy are both rough estimation and no final conclusion can be drawn on the validity of a given method by comparing calculated values to them. Furthermore, all experimental results are given for manganese dimer in matrices. We will come back to this issue and to the discrepancy between the experimental and calculated ground state later on, but first we will review and discuss the previous theoretical calculations on Mn_2.

In Table IV we compare our calculated bond length, binding energy and total spin value with previous calculations and experiment. According to the present results, Mn_2 has a ferromagnetic ground state ($\mu=10\,\mu_B$) with a bond length of 4.95 (4.75) a.u. and a binding energy of 0.63 (0.84) eV at the PBE96 [LSDA (PW91)] level. The first calcula-

TABLE IV. Calculated and experimental equilibrium bond length (r_e), harmonic frequency (ω_e), binding energy (BE), and total spin value (m_S) or electronic state of neutral manganese dimer.

	r_e	ω_e	BE	m_S/state
HF+Heisenberg[a]	5.44		0.79	$^1\Sigma_g^+$
LSDA(GL)[b]	5.03	220	1.25	5
	5.10	210	1.25	5
LSDA(JMW)[c]	3.16	729	0.98	1
	4.76	144	0.86	0 (AF)
	4.06	233	0.72	0 (AF)
G94:LSDA(VWN)[d]	3.06		1.54	1
	4.78		1.29	5
G94:BPW91[d]	4.72		0.91	5
G94:B3LYP[d]	6.71		0.06	5
DMOL:LSDA(VWN)[d]	4.75		1.15	5
	3.17		0.80	1
	4.71		0.72	0 (AF)
DMOL:BPW91[d]	4.93		0.82	5
	5.08		0.34	0 (AF)
PBE96[e]	4.93		0.99	5
	3.19		−0.41	1
	5.13		0.54	0 (AF)
LSDA(PW91)[f]	4.75	270	0.84	5
	3.15		0.57	1
	4.65		0.53	0 (AF)
PBE96[f]	4.95	190	0.63	5
	3.20		1.00	1
	5.10		−0.19	0 (AF)
Expt.	6.42[g]	76.42[h]	≤0.8[i]	$^1\Sigma_g^{+j}$

[a]Results from Ref. 11. HF+Heisenberg: Approximate Hartree–Fock+Heisenberg exchange treatment.
[b]Results from Ref. 36. GI: Gunnarsson and Lundqvist functional (Ref. 55).
[c]Results from Ref. 37. JMW: Janak, Moruzzi, and Williams functional (Ref. 56).
[d]Results from Ref. 12. BPW91: Becke exchange (Ref. 52) and Perdew–Wang correlation functionals (Ref. 19). B3LYP: Becke 3 parameters functional (Ref. 54). G94 (Ref. 40) and DMOL (Ref. 41) designate the program used.
[e]Results from Ref. 13. PBE96: Perdew, Burke, and Ernzerhof functional (Ref. 20).
[f]Present work.
[g]Estimation in krypton matrix, from Ref. 8.
[h]In krypton matrice, from Ref. 31.
[i]Estimation. From Ref. 35.
[j]From Refs. 6 and 7.

tions on Mn_2 were performed by Nesbet.[11] Using an approximate Hartree–Fock calculation including Heisenberg exchange interaction, he had predicted a weakly bound antiferromagnetic dimer with a long bond length. Harris and Jones,[36] have performed nonbroken symmetry calculations at the LSDA(GL) level and have found a weakly bound ferromagnetic ground state with a long bond length. They have in fact found two degenerate solutions, both of them are reported in Table IV. Salahub and Baykara[37,38] only explored a few spin configurations. The lowest reported state is the weakly bound ferromagnetic ''triplet,'' with a short bond length. They have found three electronic states within 0.3 eV (note that the two ''singlet'' as the two ''11-tuplet'' of Harris and Jones, were obtained by forced occupation of symmetry adapted orbitals). Salahub[38] have argued that the existence of those states cannot be accounted by the various spin states of an Heisenberg manifold. We share the same general conclusion but we will come back to this point later. We have also found a ferromagnetic ''triplet'' at approximately the same bond length (3.15 a.u.) bound by 0.57 eV at the LSDA (PW91) level in good agreement with their results. We can reasonably assume that if they had explored higher spin configuration they might probably had found a ferromagnetic $m_S=5$ ground state. Bauschlicher[39] has performed single point calculations on the neutral dimer at the CASSCF level using a limited active space. Bauschlicher found the $^1\Sigma_g^+$ state 0.013 eV more stable than the $^{11}\Sigma_u^+$ state at 5.5 a.u. yielding a J value of -7 cm^{-1}. But at 6.5 a.u., the $^{11}\Sigma_u^+$ state is 0.002 eV more stable. He has also underlined that these results might not be reliable considering the failure of CASSCF calculations on the chromium dimer but mainly because the chosen basis set is not suited for van der Waals interactions.

Very recently, Nayak and Jena[12] have performed LSDA (VWN) and GGA(BPW91) calculations on small Mn_n ($n=2-5$) clusters. They have found that all clusters are ferromagnetically coupled and carry a magnetic moment of 10, 15, 20, and 25 μ_B, respectively. We will concentrate our interest on their dimer results. They have mostly reported three different states for the dimer: the ferromagnetic ''11-tuplet,'' the ferromagnetic ''triplet'' (identical to the one of Salahub and Baykara) and, when possible, the antiferromagnetic ''singlet.'' They have performed calculations with two programs, namely GAUSSIAN 94 (Ref. 40) and DMOL (Ref. 41). No antiferromagnetic solutions were reported with GAUSSIAN 94 since, according to the authors, it does not offer this option. Their DMOL LSDA (VWN) results are in good agreement with our LSDA (PW91) results and give the long bond length ferromagnetic ''11-tuplet'' as the ground state. On the other hand, GAUSSIAN 94 LSDA (VWN) yield a ''triplet'' ground state with a short bond length (3.06 a.u.) bound by 1.54 eV. The discrepancy between GAUSSIAN and DMOL LSDA (VWN) results is intriguing. Is it related to a basis set problem (GAUSSIAN calculations were done with an Hartree–Fock optimal basis set) or does it point out an error in one of the two programs? DMOL and GAUSSIAN GGA (BPW91) results are in good agreement with our GGA (PBE96) calculations. They thus predict the long bond ferromagnetic ''11-tuplet'' as the ground state and their binding energy are in the same range as ours. Finally, while their results using B3LYP functional predicted the ferromagnetic ''11-tuplet'' as the ground state, the optimal bond length is very long compared to ours and the binding energy is very small. In this regard, we would like to point out that Scheiner *et al.*[42] have shown that three parameter functionals are more sensitive than other methods to the size of the basis set. In fact, properties converge only for very large basis sets like the correlation-consistent basis set of Dunning and co-workers.[43] Furthermore, as it can be seen in Fig. 11, the B3LYP functional completely fail to correctly describe the binding in chromium dimers. One thus wonders if the B3LYP results are reliable. Though these results are in good agreement with the experiment, as we have stated before, since the experimental parameters are estimated values in matrices, a straightforward comparison will not necessarily indicate which theoretical method is better.

At the same time as Nayak and Jena, Pederson *et al.*[13]

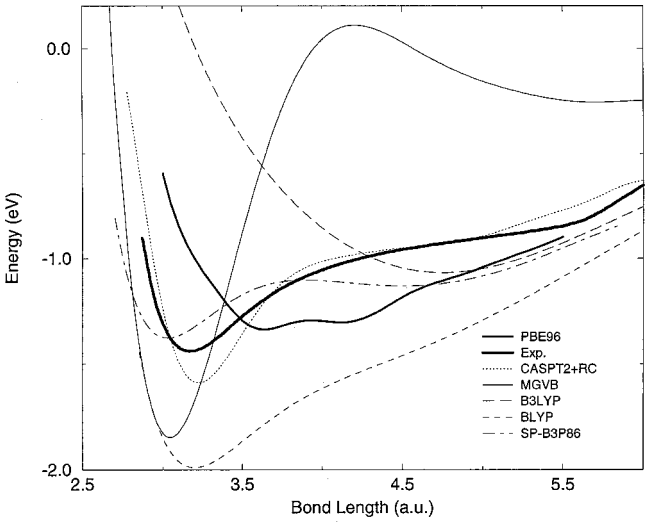

FIG. 11. Several theoretical potential energy curves of the Cr_2 dimer.

have published GGA (PBE96) results on Mn_n $(n=2-8)$ clusters. The general trends in the two studies are similar. Their PBE96 results on the neutral dimer are in agreement with our results. The bond length and relative energies (except for the $m_S=0$ paramagnetic state which is 0.53 eV less stable in our case) of the different spin states are identical to ours, though the absolute binding energies differ by 0.36 eV. This difference is attributed to the way the atom was calculated. It is comforting to note that two different implementations of KS-DFT using the GGA (PBE96) functional and two different optimal DF basis sets, leads to the same results for all spin values considered. These authors also report calculations using the Bachelet, Hamann, and Schlüter[44] pseudopotential, but these pseudopotentials are not suited for spin polarized systems.

We now come back to the discrepancy between our (as well as others[12,13]) predicted ferromagnetic ground state of free Mn_2, and the experimental predicted antiferromagnetic ground state. This discrepancy can be due to two reasons. Since the experiments are carried out on dimers in matrices and the theoretical studies are based on free clusters, one could argue that it is probably the matrix which changes the magnetic coupling. ESR experiments on several matrices (Ar, Kr, Xe, cyclopropane) show that the matrix has a minor effect on the measured properties.[6,8,10] This either implies that the matrix has no effect or all matrices have the same effect. This can be resolved by performing Stern–Gerlach experiments on free Mn_n clusters. Such attempts have, however, failed since Mn_2 is a weakly bound dimer and it is difficult to produce them under ordinary experimental conditions though recent experiments using a cryogenic cluster source indicate that it might still be possible.[45] We would only like to add that the energy difference between the ferromagnetic and antiferromagnetic states is 0.44 eV and it is difficult to imagine that a matrix could invert the ordering of states which differ by such a large energy difference. The second source of discrepancy could be that the experiments are analyzed by assuming a Heisenberg Hamiltonian, whereas we show in Fig. 4, the binding energy of different spin states first decreases and then increases as the spin is increased.

In contrast to Mn_2, the ESR experiments on Mn_2^+[14] indicate a ferromagnetically coupled dimer with $\mu=11\,\mu_B$. Experimental estimates of the binding energy range from 0.85 ± 0.2 eV[46] to $\geqslant 1.39$ eV.[47] The present value of 1.63 (1.81) eV at the PBE96(LSDA(PW91)) level lies within the experimental range. Bauschlicher[39] have also obtained a ferromagnetic ground state with $\mu=11\,\mu_B$, $r_e=6.060(5.848)$ a.u. and $D_e=1.09(1.26)$ eV at the CASSCF (CISD) levels of theory. At the CASSCF level, Bauschlicher found the relative stability of the spin states ranging from $S=4.5$ to $S=0.5$ to be 0.09, 0.17, 0.26, 0.35, and 0.44 eV higher than the ground state, respectively. The corresponding bond lengths are 6.066, 6.072, 6.078, 6.082, 6.087 a.u., respectively. This is to be compared to our results of 0.19 (4.70), 1.67 (4.10), 1.78 (4.35), and 0.39 eV (5.10 a.u.), respectively, at the PBE96 level. According to these results, GGA leads to relatively short bond lengths and large energy spacing. Furthermore, instead of having a regular progression of the relative stability and bond length with the spin variation, we have a nonmonotonic progression as seen from Fig. 5. Since Cr_2 calculations have already cast doubt on majority of theoretical methods (except CASPT2 calculations) we cannot unambiguously say which theoretical predictions are better. We also note that our calculated ground state of Mn_2 is also ferromagnetic with a net magnetic moment $(\mu=10\,\mu_B)$ smaller than the one of Mn_2^+. The trend continues with Mn_2^-, we find a ferromagnetic ground state with $\mu=9.0\,\mu_B$. It has a bond length of 4.40 a.u. and a binding energy of 1.67 eV. Both the cationic and the anionic dimers are, therefore, more stable than the neutral. In the case of Mn_2^-, we observe a *Z*-type evolution of the binding energy (see Fig. 6) with increasing m_S values. Surprisingly, the highest spin state possible $m_S=5.5$, is not the most stable.

C. Neutral and charged Cr–Mn dimers

In this section we breifly discuss our results on CrMn dimers and compare them to the only available experimental data. ESR experiments[10] on CrMn in matrices found that the molecule has a total spin of $S=1.5$ indicating a net magnetic moment. Our studies on the free dimer indicate that the ground state is ferrimagnetic: atoms have antiferromagnetically coupled spins of different magnitude at the two sites with a net spin of $m_S=0.5$. This shows that even though CrMn and Mn_2^+ have the same number of electrons, their coupling is different which might be expected considering that their external potential are different. The molecule has a bond length of 4.30 a.u. and a binding energy of 0.82 eV within the GGA (see Table II). In contrast to neutral CrMn dimers, we find that both the cation and the anion have an antiferromagnetic ground state with a total net spin of zero. Charged dimers are also significantly more stable than the neutral dimer. As for Cr_2 and Mn_2, the evolution of the BE of the charged and neutral CrMn dimers with m_S is nonmonotonic and neither quadratic. Furthermore, the variation of the bond length with m_S are ranging from 3.5 to 5.8 a.u.

(see Figs. 7–9). Again, this kind of behavior cannot be explained by a simple Heisenberg Hamiltonian.

IV. CONCLUSIONS

To summarize, we have shown that the current density functional theory, while providing a reasonable overall description of the electronic structure and the nature of magnetic coupling in dimers, does need further development to properly describe pure spin states. Our results show that while the coupling in Cr_2 changes with ionization, neutral and charged Mn_2 molecules are all ferromagnetic. In CrMn molecules, the coupling changes from ferrimagnetic in neutral to antiferromagnetic in charged dimers. In case of Mn_2^+ and CrMn we find that while both the dimers have the same number of electrons, their coupling is very different showing that the details of the electronic structure are important. Finally, our results on Mn_2 show that it cannot be described within a simple Heisenberg model.

The most intriguing features that come out when comparing our results to the experimental results of Weltner and co-workers, is the relative energy range of the different spin states. While they observed energy spacing of 0.001 to 0.017 eV, our relative energies range from 0.44 to 1.79 eV. The only way we could think of to reconciliate both predictions is to assume either that the matrix effects are more important than we might expect or the experimental analysis based on a Heisenberg Hamiltonian has limitations.

ACKNOWLEDGMENTS

N.D. and F.A.R. are grateful to the Swiss National Science Foundation for financial support. S.N.K. is grateful to the Department of Energy (DE-FG05-96ER45579) for financial support. N.D. would like to thanks J.-L. Helfer, D. Gerion, and S. Fedrigo for helpful discussions.

[1] S. P. Walch, C. W. Bauschlicher, Jr., B. O. Roos, and C. J. Nelin, Chem. Phys. Lett. **103**, 175 (1983).
[2] M. M. Goodgame and W. A. Goddard III, Phys. Rev. Lett. **54**, 661 (1985).
[3] B. Delley, A. J. Freeman, and D. E. Ellis, Phys. Rev. Lett. **50**, 488 (1983).
[4] N. A. Baykara, B. N. McMaster, and D. R. Salahub, Mol. Phys. **52**, 891 (1984).
[5] G. S. Painter, J. Phys. Chem. **90**, 5530 (1986).
[6] R. J. Van Zee, C. A. Baumann, and W. Weltner, Jr., J. Chem. Phys. **74**, 6977 (1981).
[7] J. C. Rivoal, J. Shakhs Emanpour, K. J. Zeringue, and M. Vala, Chem. Phys. Lett. **92**, 313 (1982).
[8] C. A. Baumann, R. J. Van Zee, S. V. Bhat, and W. Weltner, Jr., J. Chem. Phys. **78**, 190 (1983).
[9] M. Cheeseman, R. J. Van Zee, and W. Weltner, Jr., J. Chem. Phys. **91**, 2748 (1989).
[10] M. Cheeseman, R. J. Van Zee, H. L. Flanagan, and W. Weltner, Jr., J. Chem. Phys. **92**, 1553 (1990).
[11] R. K. Nesbet, Phys. Rev. **135**, A460 (1964).
[12] S. K. Nayak and P. Jena, Chem. Phys. Lett. **289**, 473 (1998).
[13] M. R. Pederson, F. Reuse, and S. N. Khanna, Phys. Rev. B **58**, 5632 (1998).
[14] R. J. Van Zee and W. Weltner, Jr., J. Chem. Phys. **89**, 4444 (1988).
[15] W. J. Hehre, L. Radom, P. von R. Schleyer, and J. A. Pople, *Ab Initio Molecular Orbital Theory* (Wiley, New York, 1986).
[16] W. Kohn and L. J. Sham, Phys. Rev. **140**, A1133 (1965).
[17] F. Reuse, S. N. Khanna, V. de Coulon, and J. Buttet, Phys. Rev. B **41**, 11743 (1990).
[18] N. Godbout, D. R. Salahub, J. Andzelm, and E. Wimmer, Can. J. Chem. **70**, 560 (1992); C. Sosa, J. Andzelm, B. C. Elkin, E. Wimmer, K. D. Dobbs, and D. A. Dixon, J. Phys. Chem. **96**, 6630 (1992).
[19] J. P. Perdew and Y. Wang, Phys. Rev. B **45**, 13244 (1992).
[20] J. P. Perdew, K. Burke, and M. Ernzerhof, Phys. Rev. Lett. **77**, 3865 (1996).
[21] T. Ziegler and A. Rauk, Theor. Chim. Acta **43**, 261 (1977).
[22] V. E. Bondybey and J. H. English, Chem. Phys. Lett. **94**, 443 (1983).
[23] C.-H. Su, D. A. Hales, and P. B. Armentrout, Chem. Phys. Lett. **201**, 199 (1993).
[24] S. M. Casey and D. G. Leopold, J. Phys. Chem. **97**, 816 (1993).
[25] K. E. Edgecombe and A. D. Becke, Chem. Phys. Lett. **244**, 427 (1995).
[26] H. Cheng and L. S. Wang, Phys. Rev. Lett. **77**, 51 (1996).
[27] K. Andersson, B. O. Roos, P.-Å. Malmqvist, and P.-O. Widmark, Chem. Phys. Lett. **230**, 391 (1994).
[28] C. W. Bauschlicher, Jr. and H. Partridge, Chem. Phys. Lett. **231**, 277 (1994).
[29] L. Noodleman, J. Chem. Phys. **74**, 5737 (1981); L. Noodleman and E. R. Davidson, Chem. Phys. **109**, 131 (1986).
[30] A. Bencini, F. Totti, C. A. Daul, K. Doclo, P. Fantucci, and V. Barone, Inorg. Chem. **36**, 5022 (1997).
[31] K. D. Bier, T. L. Haslett, A. D. Kirkwood, and M. Moskovits, J. Chem. Phys. **89**, 6 (1988).
[32] A. Kant, S.-S. Lin, and B. Strauss, J. Chem. Phys. **49**, 1983 (1968).
[33] T. L. Haslett, M. Moskovits, and A. L. Weitzman, J. Mol. Spectrosc. **135**, 259 (1989).
[34] K. A. Gingerich, Faraday Symp. Chem. Soc. **14**, 109 (1980).
[35] M. D. Morse, Chem. Rev. **86**, 1049 (1986).
[36] J. Harris and R. O. Jones, J. Chem. Phys. **70**, 830 (1979).
[37] D. R. Salahub and N. A. Baykara, Surf. Sci. **156**, 605 (1985).
[38] D. R. Salahub, in *Ab Initio Methods in Quantum Chemistry-II*, edited by K. P. Lawley (Wiley, New York, 1986), p. 447.
[39] C. W. Bauschlicher, Jr., Chem. Phys. Lett. **156**, 95 (1989).
[40] M. J. Frisch *et al.*, GAUSSIAN 94 Inc. Pittsburg, PA, 1995.
[41] DMOL Code, Biosym Technologies, San Diego, CA.
[42] A. C. Scheiner, J. Baker, and J. W. Anzelm, J. Comput. Chem. **18**, 775 (1997).
[43] T. H. Dunning, J. Chem. Phys. **90**, 1007 (1989); R. A. Kendall, T. H. Dunning, and R. J. Harrison, *ibid.* **96**, 6796 (1992); D. E. Woon and T. H. Dunning, J. Chem. Phys. **98**, 1358 (1993).
[44] G. B. Bachelet, D. R. Hamann, and M. Schlüter, Phys. Rev. B **26**, 4199 (1982).
[45] G. M. Koretsky and M. B. Knickelbein, J. Chem. Phys. **106**, 9810 (1997).
[46] K. Ervin, S. K. Loh, N. Aristov, and P. B. Armentrout, J. Phys. Chem. **87**, 3593 (1983).
[47] M. F. Jarrold, A. J. Illies, and M. T. Bowers, J. Am. Chem. Soc. **107**, 7339 (1985).
[48] C. E. Moore, Analysis of optical spectra. NSRDS-NBS 34, Office of Standard Data, National Bureau of Standards, Washington, DC.
[49] H. Hotop and W. C. Lineberger, J. Phys. Chem. Ref. Data **14**, 731 (1985).
[50] U. van Barth and L. Hedin, J. Phys. C **5**, 1629 (1972).
[51] S. H. Vosko, L. Wilk, and M. Nusair, Can. J. Phys. **58**, 1200 (1980).
[52] A. D. Becke, Phys. Rev. A **38**, 3098 (1988).
[53] C. Lee, W. Yang, and R. G. Parr, Phys. Rev. B **37**, 785 (1988).
[54] A. D. Becke, J. Chem. Phys. **98**, 5648 (1993).
[55] O. Gunnarsson and B. I. Lundqvist, Phys. Rev. B **13**, 4274 (1976).
[56] J. F. Janak, V. L. Moruzzi, and A. R. Williams, Phys. Rev. B **12**, 1257 (1975).